UCRL-JRNL-224696

Phase separation in H2O:N2 mixture - molecular dynamics simulations using atomistic force fields

A. Maiti, R. Gee, S. Bastea, L. Fried

September 25, 2006

Journal of Chemical Physics

Disclaimer

Phase separation in H_2O:N_2 mixture – molecular dynamics simulations using atomistic force fields

Amitesh Maiti,* Richard H. Gee, Sorin Bastea, and Laurence E. Fried

Lawrence Livermore National Laboratory, University of California, CA 94551

Abstract

A class II atomistic force field with Lennard-Jones 6-9 nonbond interactions is used to investigate equations of state (EOS) for important high explosive detonation products N_2 and H_2O in the temperature range 700-2500 K and pressure range 0.1-10 GPa. A standard 6^{th} order parameter-mixing scheme is then employed to study a 2:1 (molar) H_2O:N_2 mixture, to investigate in particular the possibility of phase-separation under detonation conditions. The simulations demonstrate several important results, including: (i) the accuracy of computed EOS for both N_2 and H_2O over the entire range of temperature and pressure considered; (ii) accurate mixing-demixing phase boundary as compared to experimental data; and (iii) the departure of mixing free energy from that predicted by ideal mixing law. The results provide comparison and guidance to state-of-the-art chemical kinetic models.

Keywords: Supercritical phase separation, Molecular Dynamics, Equation of state

* E-mail: maiti2@llnl.gov

I. Introduction

Supercritical phase separation of fluid mixtures is an important phenomenon relevant to many fields of science and engineering [1-4]. The details of a pressure-volume-composition (P-V-x) coexistence surface are important in a number of applications including, planetary and geo-chemistry, chemical processing, toxic waste disposal, and detonation physics. The equation of state (EOS) of several binary fluid systems over limited phase space has been obtained from experimental PVT data [4]. However, it is often difficult and expensive to perform experiments, especially for mixtures containing more than two components, and at high temperatures and pressures even for simple binary mixtures.

Phase separation in a water-nitrogen mixture, the topic of the present study, has been proposed as an important phenomenon in detonation physics [5]. The detonation of typical explosives containing C, H, N, and O atoms produces a mixture of N_2, H_2O, CO_2, and other minor species at high temperatures (T = 1000-5000 K) and pressures (P = 1-100 GPa). It has long been surmised that supercritical phase separation under these extreme conditions may significantly impact the detonation characteristics [1]. Such phase separations in a H_2O:N_2 mixture have been experimentally demonstrated -- first on a 3:1 (molar) mixture by Japas, *et al.* [6] at P< 0.25 GPa, and later at higher temperatures and pressures (using a diamond anvil cell) on a 3:1 mixture by Costantino and Rice [7], and on a 2:1 mixture by van Hinsberg, *et al.* [8]. The temperature and pressure in these experiments were limited to the range T < 825 K and P < 5 GPa.

Molecular-level interactions play a crucial role in determining the EOS and phase diagrams of both single fluids and mixtures. Many theoretical models and simulations of detonation conditions neglect the internal structure of molecules and replace it with a single spherical potential, typically a Lennard-Jones 6-12 or a modified Buckingham exponential-6 form. This approach allows in particular the computation of the free-energy of single fluids using either variational or perturbational methods that employ the hard-sphere fluid as a reference system. Using an effective one-component fluid approximation for the mixture and suitable mixing rules for the unlike-pair interactions the free energy of a mixture can also be reliably calculated, which makes possible for example the calculation of solubility isotherms of binary mixtures. Using such an approach, Ree [1, 9] modeled a N_2:H_2O mixture by exponential-6 potentials and predicted phase separation at T = 4000 K and P = 33 GPa. Using a

similar potential, Koshi and Matsui [10] carried out MD simulations at $T = 2000$K and observed phase separation to occur at a density of $\rho = 1.35$ g/cc ($P \sim 6.3$ GPa).

Based on statistical mechanics arguments [11, 12] one can expect the spherical potential to be a good approximation for nonpolar molecules at high T and P, as has been verified by excellent agreement of EOS for N_2, CH_4, and CO_2 with experimental data [13]. However, for polar molecules (H_2O, NH_3, CO) the nonpolar spherical potential is not a good representation, even at the high temperatures and pressures typical of most detonation environments, and ad hoc approximations such as temperature-dependent potentials [9] or multi-species representations [14, 15] need to be used. Moreover, the driving force for phase separation in nonpolar-polar mixtures such as N_2-H_2O is likely the intrinsic dipole moment itself [16], which is averaged out in any spherical approximation [17]. In order to account for phase separation in such models, additional, hard-to-justify assumptions, such as non-additivity of the unlike pair interaction [9] become necessary. This casts doubt on the reliability of theoretical predictions obtained using such models, particularly as far as direct comparison with experimental data is concerned.

The best avenue to bridge the gap between experiment and theory, and to assist in further developments of modern thermochemical codes such as CHEETAH [14] is to model these systems in full atomistic detail using classical MD simulations. The molecular modeling literature abounds with examples of force fields developed for many different kinds of materials [18, 19]. The most accurate force fields, known as second-generation or class II force fields [19] are especially relevant to HE denotation products. Such force fields usually have a large number of parameters, both intra- and inter-molecular, which are fit to accurate quantum mechanical calculations as well as to some experimental data. These parameters are usually developed for not-so-extreme conditions of temperature and pressure, and therefore might need modifications for simulations under detonation conditions. For instance, in order to describe bond-breaking and ionization processes that may occur under extreme conditions, one needs to take recourse to so-called reactive force fields [20, 21]. The purpose of this paper, however, is to explore the accuracy of standard class II force fields at T and P conditions much higher than what they are typically parameterized at.

In this paper we use the class II force field COMPASS [22] and show that it is able to generate accurate equations of state for pure H_2O and N_2 over a wide range of temperatures and pressures. We

then study a 2:1 (molar) H_2O:N_2 mixture, and investigate the mixing-demixing phase boundary in the temperature range 700-1500 K using a standard 6th power parameter combination rule. We show that the phase boundary is in excellent agreement with available experimental data, and therefore can guide further developments in the mixture thermodynamics theory employed by chemical equilibrium calculations.

II. Force Field Details

Most force fields generally make a distinction between bonded (or valence) terms that operate only within the same molecule, and non-bond terms that operate between atoms belonging to different molecules, or between atoms within the same molecule separated by a few bonded neighbors. The bonded terms typically are functions of bond-lengths, angles, dihedrals, out-of-plane angles, and cross-terms. Modeled after previously developed type II force fields like CFF [23], COMPASS [22] represents bond energy terms for both N_2 and H_2O in the quartic functional forms:

$$E_{bond}(b) = K_2^{bond}(b-b_0)^2 + K_3^{bond}(b-b_0)^3 + K_4^{bond}(b-b_0)^4$$

The above is the only relevant bonded (i.e. valence) term for N_2. For water, in addition to the above bonded term for the OH bonds, one requires an angle term, which is also taken to be of the quartic form:

$$E_{angle}(\theta) = K_2^{angle}(\theta-\theta_0)^2 + K_3^{angle}(\theta-\theta_0)^3 + K_4^{angle}(\theta-\theta_0)^4 ,$$

In addition, a bond-bond and a bond-angle cross-term are also included (for water):

$$E_{bond-bond}(b,b') = K^{bond-bond}(b\ -b_0)(b'-b_0')\ ,\ \text{and}$$

$$E_{bond-angle}(\theta,b) = K^{bond-angle}(\theta-\theta_0)\{(b-b_0)+(b'-b_0')\}$$

However, the most important interactions that govern the EOS of the pure phases as well as the mixtures are the non-bond interactions, i.e., the coulombic and van der Waals interactions. The coulombic term is of the standard (unscreened) form:

$$E_{coulomb}^{ij} = \frac{q_i q_j}{r_{ij}},$$

where q_i and q_j are partial charges on atoms i and j and r_{ij} is the distance between the two atoms. The van der Waals interaction between like atoms is chosen to be of the Lennard-Jones 9-6 form:

$$E_{vdw}(r) = \varepsilon_{LJ}\left[2(r_0/r)^9 - 3(r_0/r)^6\right],$$

while the parameters for unlike atoms α and β are obtained from 6th order mixing rules [24]:

$$r_0^{\alpha\beta} = \left[\frac{1}{2}\{(r_0^{\alpha})^6 + (r_0^{\beta})^6\}\right]^{1/6}, \text{ and}$$

$$\varepsilon_{LJ}^{\alpha\beta} = 2\sqrt{\varepsilon_{LJ}^{\alpha}\varepsilon_{LJ}^{\beta}}\left[\frac{(r_0^{\alpha})^3(r_0^{\beta})^3}{(r_0^{\alpha})^6 + (r_0^{\beta})^6}\right].$$

Following standard convention we turn off non-bond interactions between bonded neighbors and bonded second neighbors, which imply that both for H_2O and N_2 the non-bond interactions operate only at the inter-molecular level. In addition, with no charge on the N-atoms, the coulomb interactions are present only between H_2O molecules. The COMPASS parameters were developed to accurately reproduce not only the structural and vibrational data of isolated molecules, but for condensed phase properties (e.g., density, cohesive energy) as well. The parameters have been validated for a large number of (mostly) organic compounds encompassing both macro- and small-molecule systems [22, 25, 26], which include liquid N_2 [22] and water [26] under ambient conditions.

Classical molecular dynamics (MD) simulations using the above force field are performed using LAMMPS [27]. *NVT* dynamics (i.e. constant system density) are carried out on a cubic simulation supercell, using the Nosé-Hoover thermostat with a time step of 1 fs. Periodic boundary conditions are employed, and both the coulomb and van der Waals contributions to the total potential energy evaluated through Ewald summation using the particle mesh Ewald technique [28]. For each phase point an equilibration run of 50000 steps (50 ps) on an initially randomized system is followed by a production run of $6\text{x}10^5$ steps (0.6 ns), and the average pressure computed. The number of molecules in our simulation cell depends on the system under investigation. Thus for pure systems a size of 1200 molecules seemed to suffice both for N_2 and H_2O (i.e., the results with larger system size, e.g., 1600

were essentially identical within statistical errors). Even for mixtures, a total of 1200 molecules appeared to yield accurate mixing-demixing phase boundary using the procedure described in section IV. However, to study the details of the phase separation dynamics, e.g., the time evolution of the domain size as well as the pressure and energy relaxation time scales, much larger systems (up to 259200 molecules) and longer simulation times (up to 4 ns) became necessary.

III. Pure systems

In Fig. 1 we display the MD results for pure N_2 and compare with predictions from an exponential-6-based thermodynamic theory [14] parameterized by matching both equilibrium and shock wave experimental data. We also include experimental data at 673 K [29] to compare with the 700 K simulated isotherm. Additionally, using MD simulation results at different temperatures we have estimated a few thermodynamic points satisfying the Hugoniot condition:

$$E - E_0 = \frac{P + P_0}{2}(V_0 - V),$$

which connects the (non-bond) energy, pressure, and volume (E, P, V) of the shocked state with the corresponding values (E_0, P_0, V_0) of the initial, unshocked one. In the inset we show the MD-estimated Hugoniot (unfilled diamonds) together with two sets of shock wave data (unfilled squares [30] and circles [31]). We conclude that the force field parameters used in our MD provide a realistic representation of N_2 for pressures up to at least 10 GPa and temperatures as high as a few thousand K, covering most of the thermodynamic region corresponding to non-dissociated supercritical fluid nitrogen. This is remarkable, considering that the force field parameters were originally developed by fitting low to room-temperature and low-pressure (1 atm) data.

H_2O is a more interesting but more difficult case since it is harder to model with a consistent thermodynamic theory. Therefore, we compare the MD-computed values with experimental data [32, 33] from various sources, available for pressures up to ~ 3 GPa. As can be seen, the agreement is excellent for the entire temperature-pressure range of the experimental data. We also find that thermodynamic predictions that empirically account for the dipole moment of water [9] can be made to

agree with experimental data only over limited ranges of pressure and temperature. In order to avoid the limitations of these approaches, newer developments that treat the dipole moment explicitly are currently being pursued [34], and MD simulations such as reported here are expected to be a valuable guide.

IV. H_2O:N_2 mixtures

Available experimental data on 3:1 and 2:1 molar mixtures of H_2O:N_2 indicate no mixing below T ~ 600 K, and a monotonic increase in the critical pressure above which the system phase separates, as indicated in Fig. 3(a). Previous theoretical calculations [1] suggest the possibility of phase separation at much higher temperatures and pressures, but the theory is not accurate enough to make a direct comparison with lower-T experimental data limited to $T < 825$ K. It is therefore of interest to study this mixture using MD simulations and compare with available experimental data.

Just like the pure phase we perform *NVT* dynamics on a cubic simulation cell of 1200 molecules representing a 2:1 (molar) mixture of H_2O:N_2, i.e., 800 H_2O and 400 N_2 molecules in the cell. The initial configuration is a randomly mixed system, which is allowed to evolve through *NVT* dynamics at a fixed T and ρ. Following a total MD run of $6\text{x}10^5$ steps (i.e. 0.6 ns), we compute the intermolecular diagonal and cross pair correlation functions $g_{\alpha\beta}(r)$ for all N and O *atoms* (i.e., α or β is either N or O), and from that the average coordination numbers $n_{\alpha\beta}(R)$ and local number fractions $x_{NN}(R)$ and $x_{OO}(R)$, as defined below [35]:

$$n_{\alpha\beta}(R) = 4\pi\rho_N x_\beta \int_0^R r^2 g_{\alpha\beta}(r)dr \text{ , where } \alpha, \beta = \text{N or O} \qquad (1)$$

$$x_{NN}(R) = \frac{n_{NN}(R)}{n_{NN}(R) + n_{NO}(R)} \text{ and } x_{OO}(R) = \frac{n_{OO}(R)}{n_{OO}(R) + n_{ON}(R)}. \qquad (2)$$

In eq. (1) above, ρ_N is the total number density in the system, and x_β is the overall *number* fraction of species β, i.e., in our case of 2:1 (molar) mixture of H_2O:N_2, x_β is 0.5 for both N and O. To characterize whether a mixture is homogeneous or phase separating we consider the sum of the two local mole fractions [36],

$$x_s(R) = x_{NN}(R) + x_{OO}(R), \qquad (3)$$

which should be equal to 1 (for all R) for a completely homogeneous mixture without any spatial variation of component densities. For an inhomogeneous mixture, particles of the same kind predominate the distribution, and $x_s(R) > 1$ for R beyond the first peak of all the three pair-correlation functions g_{NN}, g_{NO}, and g_{OO}. Fig. 3(a) displays the value of the function $x_s(R)$ as a function of the overall system density ρ for a fixed temperature T = 850 K and for the choice of $R = (5/\rho)^{1/3}$, where R is in Å and ρ is in g/cc. For all densities considered, this value of R is beyond the first peak of all the $g_{\alpha\beta}$. Fig. 3(a) shows two distinct regions, a lower density region of smaller increase rate in $x_s(R)$, corresponding to a microscopically homogeneous system, and a higher density region of faster increase rate in $x_s(R)$ indicative of microscopic inhomogeneities, i.e., phase separation. The intersection of these two regions can be identified as the transition density above which phase separation occurs [10, 36]. Thus, from Fig. 3(b) the phase separation at T = 850K occurs at around a density of 1.1 g/cc, which corresponds to a pressure of 1.9 GPa, in excellent agreement with experimental data. The same procedure is followed at different temperatures, and the results are plotted in Fig. 3(a), along with the available experimental points. The theoretical results are in good agreement with the experimental data below 825 K.

The above results were obtained from 0.6 ns of MD simulation on a periodic system of 1200 molecules and provide valuable information on the phase diagram of the N_2-H_2O binary system. At the same time, to study the characteristics of phase segregation kinetics in this system, including timescales for pressure and energy equilibration, domain growth and morphology, etc., we also carried out MD simulations on a much larger ensemble consisting of 259200 molecules (691200 atoms) for a total simulation time of 4 ns. Fig. 4(a-c) display snapshots from one specific run at T = 850 K and ρ = 1.6 g/cc (P = 7.3 GPa) showing the self-similar domain evolution typical of phase separation kinetics. The

observed phase separation is in agreement with the phase boundary in Fig. 3(a). Details of this time evolution, including its dependence on the quench pressure will be published separately.

V. Departure from ideal mixing law

Determination of the mixing-demixing phase boundary from direct MD simulation, as illustrated in the previous section, involves long (~ 0.5-1 ns) MD simulations. An alternative criterion for phase separation is to compute the mixing energy defined by,

$$\Delta E_m = E(mixture) - x_{H_2O} E(H_2O) - (1 - x_{H_2O}) E(N_2) \tag{4}$$

where E is the total energy averaged over a much shorter simulation (~ 20 ps), and x_{H_2O} is the mole fraction of H_2O in the solution. One would then compare the mixing energy with a critical value to determine if the system would remain homogeneous or phase separate. In case of zero volume change upon mixing, the ideal mixing law yields the following simple expression for the critical value of the mixing energy (see Appendix):

$$\frac{\Delta E_{m,critical}}{N k_B T} = \frac{1}{2}[(1 - x_{H_2O}) \frac{v_{N_2}}{v_{H_2O}} + x_{H_2O} \frac{v_{H_2O}}{v_{N_2}}] = \frac{1}{6}[\frac{v_{N_2}}{v_{H_2O}} + 2 \frac{v_{H_2O}}{v_{N_2}}], \tag{5}$$

for our 2:1 (molar) H_2O:N_2 mixture. In the above equation, v_{N_2} and v_{H_2O} are the molar volumes of nitrogen and water respectively. So, according to the classical mixing law, the T-dependence of the critical value of ΔE_m enters only through the (T, P) dependence of the molar volume ratio v_{N_2} / v_{H_2O}. From the pure phase results of Fig.1 and 2, we find that for 700 K $\leq T \leq$ 2500 K and $0.8 \leq \rho \leq 1.8$, the ratio v_{N_2} / v_{H_2O} lies within 1.5 and 1.7, which, according to eq. (5) corresponds to only a narrow range of critical $\Delta E_m / N k_B T$ between 0.474 and 0.479. However, as illustrated in Table I, our MD simulation indicates a stronger variation of this quantity with T, with the value at higher temperatures (1500 K) approaching the ideal mixing value.

VI. Summary

Using classical MD simulations we show that a well-parameterized class II force field can reproduce experimental equations of state both for non-polar (N_2) and polar (H_2O) liquids over a wide range of temperatures and pressures relevant to detonation conditions. A standard sixth order mixing rule is shown to accurately determine mixing-demixing phase boundary. Given that experiments under extreme conditions are difficult and expensive, this provides an accurate and convenient way to extrapolate phase boundary information at higher temperatures and pressures, and can serve as a guide to systematic improvements in chemical equilibrium codes like CHEETAH [14].

VII. Acknowledgements

The work was performed under the auspices of the U.S. Department of Energy by the University of California Lawrence Livermore National Laboratory under Contract W-7405-Eng-48.

APPENDIX: Ideal mixing law

From classical ideal mixing theory (under no volume changes upon mixing) the free energy of mixing F_m of the H_2O:N_2 system is given by [37]:

$$\frac{F_m}{Vk_BT} = \frac{1}{v_1}\varphi\ln\varphi + \frac{1}{v_2}(1-\varphi)\ln(1-\varphi) + \alpha\varphi(1-\varphi) \qquad \text{(A.1)}$$

where V is the total volume of the system, k_B the Boltzmann constant, φ the *volume fraction* of H_2O, and $v_1(v_2)$ the molecular volume of H_2O (N_2) respectively. The two phases will mix if F_m is a convex function of φ, i.e. $\frac{\partial^2 F_m}{\partial\varphi^2} > 0$, which implies:

$$\alpha\varphi(1-\varphi) < \tfrac{1}{2}\left(\frac{1-\varphi}{v_1} + \frac{\varphi}{v_2}\right) \qquad \text{(A.2)}$$

The first two terms in Eq. (A.1) are related to the increase in configurational entropy due to mixing. If we relate the last term of Eq. (A.1) to the excess Enthalpy ΔH_m computed from MD simulations, which under the assumption of no volume change upon mixing is the same as excess internal energy ΔE_m, condition (2) becomes:

$$\frac{\Delta E_m}{N k_B T} < \frac{1}{2}[(1-x)\frac{v_2}{v_1} + x\frac{v_1}{v_2}] \qquad \text{(A.3)}$$

where N is the total number of molecules in the system, and we have recast the volume fractions φ and $1-\varphi$ in terms of mole fractions x and (1- x) by using the relations:

$$\varphi = \frac{x v_1}{v}, \text{ and } 1-\varphi = \frac{(1-x)v_2}{v} \quad , \qquad \text{(A.4)}$$

where $v = V/N = x v_1 + (1-x)v_2$ is the average molecular volume of the whole system.

The critical concentration is obtained by setting the third derivative $\partial^3 F_m / \partial \varphi^3 = 0$, which yields the following values of volume fraction and mole fraction at the critical point:

$$\varphi_{cr} = \frac{\sqrt{\gamma}}{1+\sqrt{\gamma}} \text{ and } x_{cr} = \frac{\gamma^{3/2}}{1+\gamma^{3/2}}, \text{ where } \gamma = \frac{v_2}{v_1}. \qquad \text{(A.5)}$$

For wide range of T and P of our interest $\gamma = v_{N_2} / v_{H_2O}$ is between 1.5 and 1.7, which implies values of x_{cr} between 0.65 and 0.69. Therefore, a H_2O:N_2 mixture in the 2:1 mole fraction ratio is expected to be close to the critical concentration.

References:

1. E. Kiran, P. G. DeBenedetti, C. J. Peters, eds., Supercritical Fluids: Fundamentals and Applications (NATO Science Series E:), Kluwer Academic Publishers (2000).

2. H. Weingartner and E.U. Frank, Angew. Chem. Int. Ed. **44**, 2672 (2005).

3. J. D. Gunton, M. San Miguel, and P. S. Sahni, in Phase Transitions and Critical Phenomena, Vol. 8, ed. by C. Domb and J. L. Lebowitz, Academic, New York, (1983).

4. J. A. Schouten, J. Phys. Condens. Matter **7**, 469 (1995), and references therein.

5. F. H. Ree, J. Chem. Phys. **84**, 5845 (1986).

6. M. L. Japas and E. U. Franck, Ber. Bunsen-Ges. Phys. Chem. **89**, 793 (1985).

7. S. Costantino and S. R. Rice, J. Phys. Chem. **95**, 9034 (1991).

8. M. G. E. van Hinsberg, R. Verbrugge, and J. A. Schouten, Fluid Phase Equilibria **88**, 115 (1993).

9. F. H. Ree, J. Chem. Phys. **81**, 1251 (1984).

10. M. Koshi and H. Matsui, Mol. Sim. **12**, 227 (1994).

11. M.S. Shaw, J.D. Johnson, and B.L. Holian, Phys. Rev. Lett. **50**, 1141 (1983).

12. J.L. Lebowitz and J.K. Percus, J. Chem. Phys. **79**, 443 (1983).

13. J.D. Johnson, M.S. Shaw, and B.L. Holian, J. Chem. Phys. **80**, 1279 (1984).

14. L.E. Fried, W.M. Howard, and P.C. Souers, Proceedings of the 12th International Detonation Symposium, San Diego, California, Aug. 11-16, 2002, p. 567.

15. L. E. Fried and W. M. Howard, J. Chem. Phys. **110**, 12023 (1999).

16. X.S. Chen, M. Kasch, and F. Forstmann, Phys. Rev. Lett. **67**, 2674 (1991).

17. D. MacGowan, D.B. Nicolaides, J.L. Lebowitz, and C.-K. Choi, Mol. Phys. **58**, 131 (1986).

18. J. R. Hill, L. Subramanian, and A. Maiti, "Molecular Modeling Techniques in Material Sciences," CRC Press, Boca Raton, Fl (2006).

19. F. Jensen, "Introduction to Computational Chemistry," John Wiley, Chichester (1999).

20. A. C. T. van Duin, S. Dasgupta, F. Lorant, and W. A. Goddard III, J. Phys. Chem. A **105**, 9396 (2001); A. C. T. van Duin *et al.*, J. Phys. Chem. A 107, 3803 (2003); Q. Zhang *et al*., Phys. Rev B **69**, 045423 (2004).

21. D. W. Brenner et al., J. Phys. Condens. Matter **14**, 783 (2002).

22. H. Sun, J. Phys. Chem. B **102**, 7338 (1998).

23. J. R. Maple, U. Dinur, and A. T. Hagler, Proc. Natl. Acad. Sci. USA **85**, 5350 (1988).

24. J. R. Durig and T. G. Sheehan, Raman Spectrosc. **21**, 635 (1990).

25. H. Sun, P. Ren, and J. R. Fried, Comput. Theor. Polym. Sci. **8**, 229 (1998); D. Rigby, H. Sun, and B. E. Eichinger, Polymer International **44**, 311 (1997); J. Yang, Y. Ren, A. Tian, and H. Sun, J. Phys. Chem. B **104**, 4951 (2000); S. W. Bunte and H. Sun, J. Phys. Chem. B **104**, 2477 (2000); M. J. McQuaid, H. Sun, and D. Rigby, J. Comput. Chem. 25, 61 (2004).

26. D. Rigby, Fluid Phase Equilibria **217**, 77 (2004).

27. See webpage: http://www.cs.sandia.gov/~sjplimp/lammps.html.

28. H. G. Peterson, J. Chem. Phys. **103**, 3668 (1995).

29. S. L. Robertson and J. S. E. Babb, J. Chem. Phys. **50**, 4560 (1969).

30. V. N. Zubarev and G. S. Telegin, Sov. Phys. Dokl. **7**, 34 (1962).

31. S. P. Marsh, LASL Shock Hugoniot Data, University of California Press, Berkeley, CA (1980).

32. W. Wagner and A. Pruss, J. Phys. Chem. Ref. Data **31**, 387 (2002).

33. J.P. Brodholt and B.J. Wood, Geochim. Cosmochim. Ac. **58**, 2143 (1994).

34. S. Bastea, K.R. Glaesemann, L.E. Fried, to be submitted to 13th International Detonation Symposium, Norfolk, VA (2006).

35. The correlation functions $g_{\alpha\beta}(r)$ are computed over a short (50 ps) trajectory following the long (0.6 ns) MD simulation. In order to ensure better statistics, we average over 10 independent short runs, each of 50 ps.

36. C. Hoheisel and U. Deiters, Mol. Phys. **37**, 95 (1979); M. Schoen and C. Hoheisel, Mol. Phys. **53**, 1367 (1984); M. Schoen and C. Hoheisel, Mol. Phys. **57**, 65 (1986).

37. See, e.g., G. H. Fredrickson, A. J. Liu, and F. H. Bates, Macromolecules **27**, 2503 (1994).

Table I. Calculated values of mixing energy ΔE_m for a few phase points on the mixing-demixing phase boundary. Temperature, density, and the corresponding pressure of each phase point are indicated.

T (K)	ρ (g/cc)	P (GPa)	$\Delta E_m / Nk_B T$
700	1.10	0.6	0.399
850	1.40	1.9	0.511
1000	1.29	3.6	0.573
1200	1.55	7.8	0.553
1500	1.90	18.8	0.497

Figure Captions:

1. Pressure-density isotherms for N_2 at three different temperatures (indicated): MD results (♦, ●, ▲) compared with thermodynamic theory predictions (◊, ○, Δ) with parameters obtained by fitting equilibrium and shock wave experimental data. Also included are some experimental data points [29] (crossed squares) at 673 K. For each isotherm a curve (fit to data represented by unfilled symbols) is drawn as a guide to the eye. *Inset:* MD-estimated Hugoniot (◊) together with two sets of shock wave data (□ [30] and ○ [31]).

2. Pressure-density isotherms for H_2O: MD results (♦, ●, ▲) compared with experimental steam data (◊, ○, Δ) (ref. [32]) for three different temperatures. Two data-points at T ~ 1500 K (□) from ref. [33] are also included. Curves for each isotherm are drawn as a guide to the eye.

3. Mixing-demixing phase boundary points computed by MD and compared with experimental data: (a) computed critical pressure for a few different temperatures, with some experimental numbers indicated. *Inset*: close-up view of experimental + MD data for T between 600K and 900K; (b) Static cross-correlation factor ($X_s - 1$) plotted as a function of density at T = 850 K, and critical pressure indicated.

4. A large-scale MD simulation (691200 atoms) at $T = 850$ K and $\rho = 1.6$ g/cc ($P = 7.3$ GPa), for a 2:1 (molar) H_2O:N_2 mixture showing progressive phase separation into N_2-rich and H_2O-rich domains: (a) Time t = 0, initial mixed state; (b) t = 1 ns; (c) t = 3 ns. Only N-atoms (blue) and O-atoms (white) are displayed for clarity.

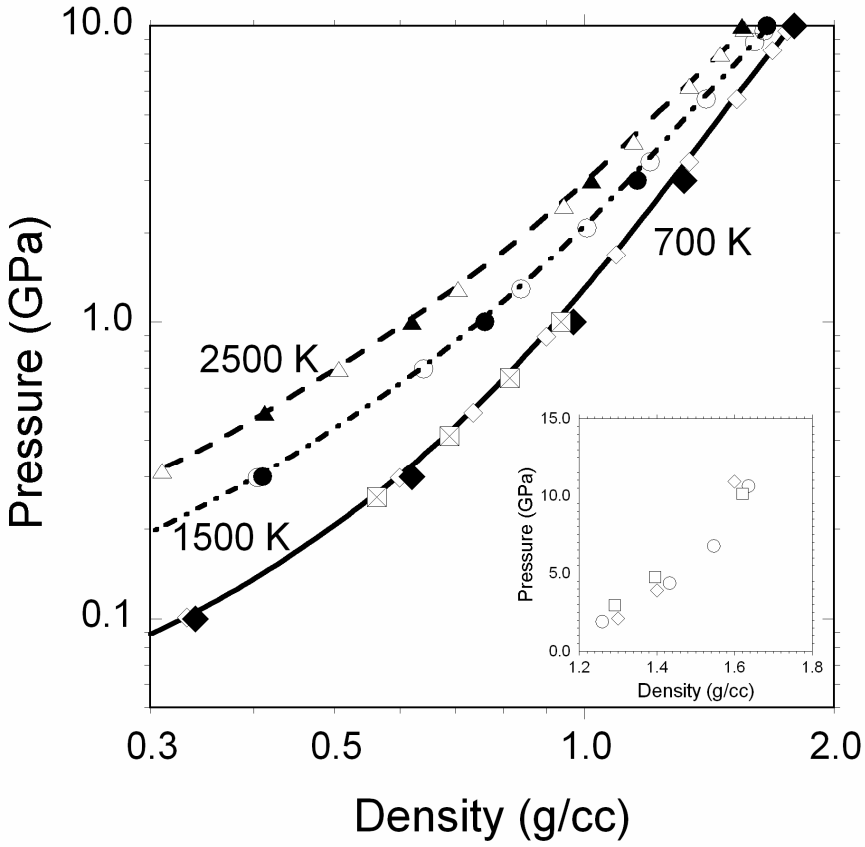
10.0
1.0
0.1
Pressure (GPa)
0.3
0.5
1.0
2.0
Density (g/cc)
2500 K
1500 K
700 K
15.0
10.0
5.0
0.0
Pressure (GPa)
1.2
1.4
1.6
1.8
Density (g/cc)

Figure 1

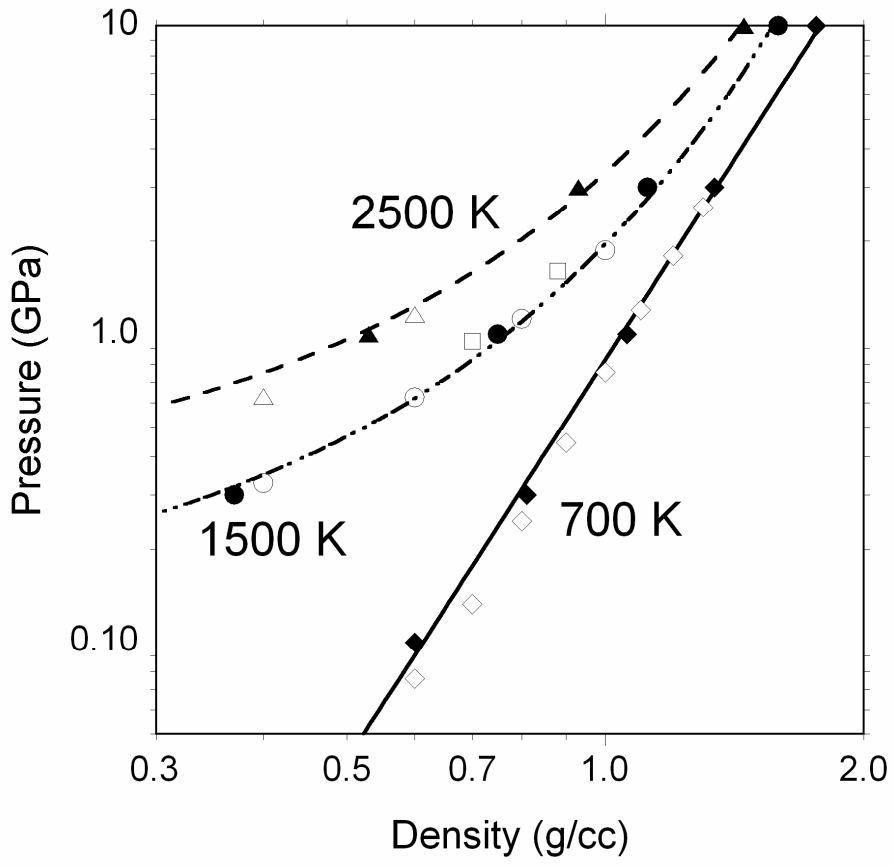
10
1.0
0.10
Pressure (GPa)
2500 K
1500 K
700 K
0.3
0.5
0.7
1.0
2.0
Density (g/cc)

Figure 2

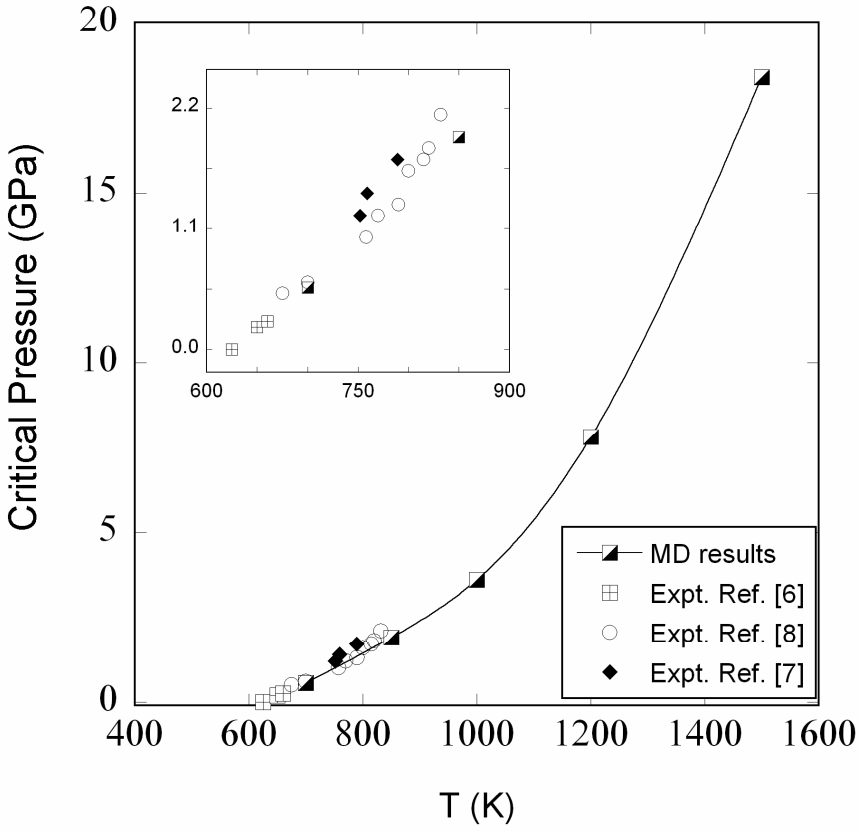
Critical Pressure (GPa)
T (K)
MD results
Expt. Ref. [6]
Expt. Ref. [8]
Expt. Ref. [7]
0
5
10
15
20
400
600
800
1000
1200
1400
1600
0.0
1.1
2.2
600
750
900

Figure 3(a)

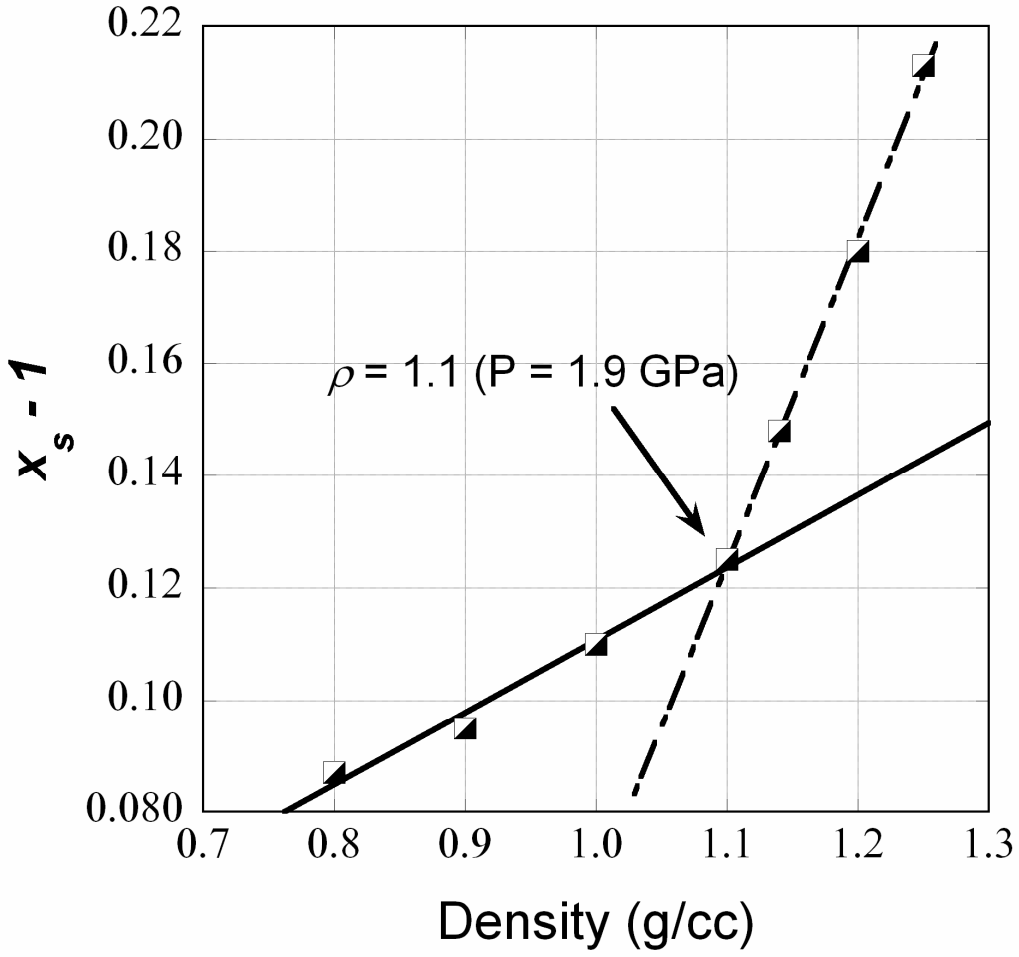
0.22
0.20
0.18
0.16
0.14
0.12
0.10
0.080
χ_s - 1
ρ = 1.1 (P = 1.9 GPa)
0.7
0.8
0.9
1.0
1.1
1.2
1.3
Density (g/cc)

Figure 3(b)

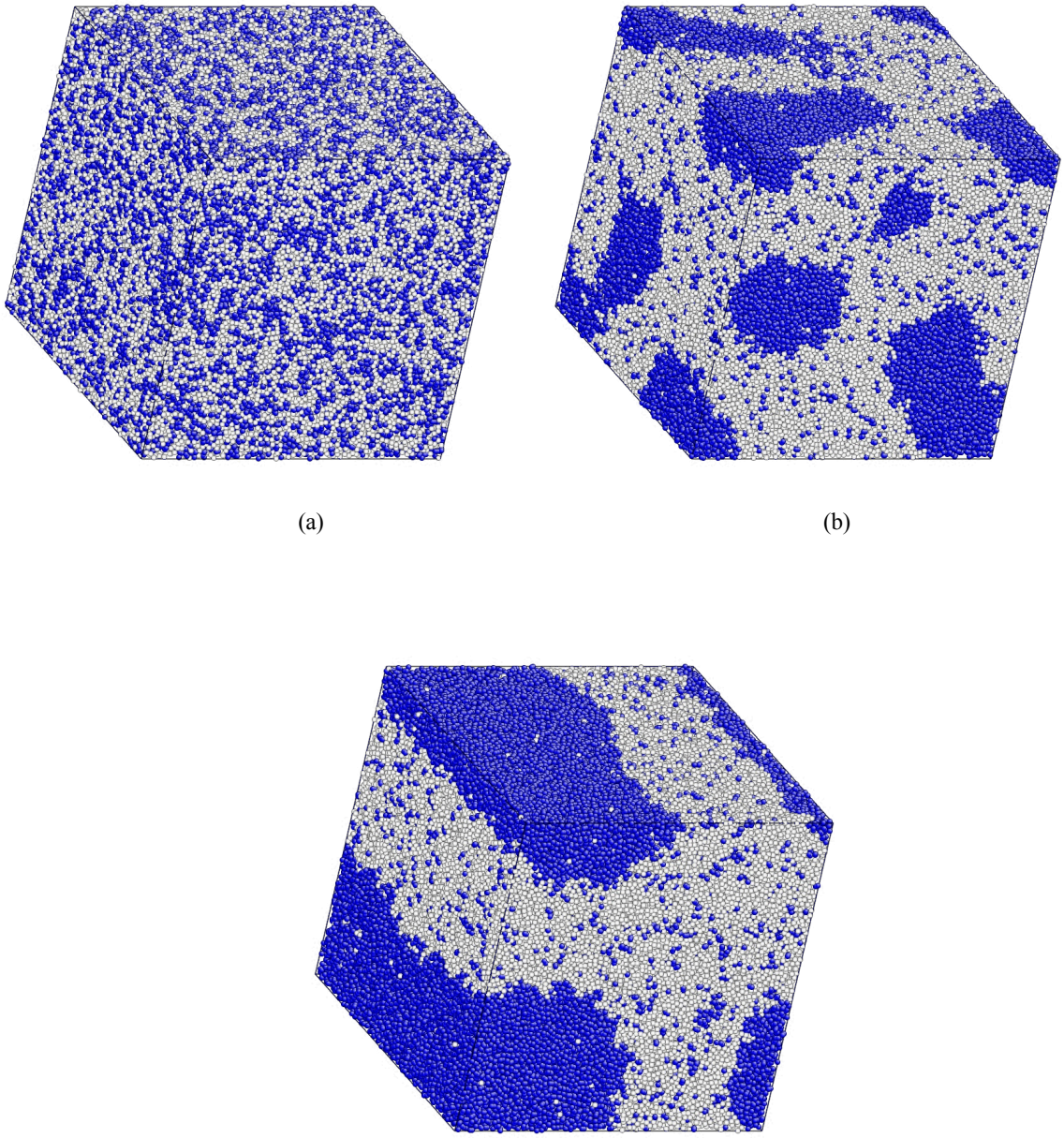

(a) (b)

(c)

Figure 4